

# Agriculture Vulnerability to Climate Change in a Snowmelt-Driven Basin in Semiarid Chile

Sebastian Vicuña<sup>1</sup>; James McPhee<sup>2</sup>; and René D. Garreaud<sup>3</sup>

**Abstract:** The Limarí River basin is one of the most important watersheds in north-central Chile (30°S). Its headwaters lie at the top of the subtropical Andes (>5,000 m above sea level) and the river flows westward into the Pacific Ocean over a length of approximately 200 km. This basin has a marked snowmelt-driven hydrological regime and, in spite of the arid conditions that characterize this region, holds more than 50,000 ha of highly productive agricultural land thanks to its irrigation infrastructure and three interconnected reservoirs. Like many semiarid regions around the world, north-central Chile is expected to become warmer and drier during the 21st century as a consequence of ongoing anthropogenic climate change. The associated reduction in streamflow, changes in hydrograph timing, and enhanced evapotranspiration will undoubtedly threaten agriculture in the Limarí basin and elsewhere in semiarid Chile. In this paper, the effect of temperature and precipitation on surface hydrology, performance of water infrastructure, and irrigation coverage in the Limarí basin is investigated by using the water evaluation and planning (WEAP) model. WEAP was calibrated by using current climate and agriculture patterns, and then forced with a set of 30-year-long climate scenarios, each of them obtained by adding a temperature and precipitation perturbation to the historical time series. This delta approach allows (1) determination of the sensitivity of selected variables to climate change, and (2) obtaining a projection of the effects in irrigation coverage expected for the near and far future (2010–2040 and 2070–2100, respectively). Both aspects are investigated for agricultural districts with varying access to irrigation infrastructure and groundwater; this exercise highlights the relevance of added storage and innovative conjunctive use of surface and groundwater resources for improving the resilience and adaptability of irrigated agriculture in the face of a changing climate. DOI: 10.1061/(ASCE)WR.1943-5452.0000202. © 2012 American Society of Civil Engineers.

**CE Database subject headings:** Climate change; Water resources; Agriculture; Arid lands; Reservoirs; Chile.

**Author keywords:** Climate change; Water resources; Vulnerability; Agriculture; Semiarid regions; Reservoir systems.

## Introduction

Most of the semiarid regions at subtropical latitudes are expected to become drier as a consequence of anthropogenic climate change projected during this century (Held and Soden 2006). This is likely to be the case in north-central Chile, the narrow strip of land between the Andes cordillera and the Pacific Ocean, where model-based climate projections consistently indicate a reduction in mean annual precipitation (down to 30% relative to current values) and an increase of surface air temperature (up to 4°C at the top of the Andes) for the 2070–2100 period under the A2 scenario (Fuenzalida et al. 2007). Note that A2 is a high-range scenario with

CO<sub>2</sub> concentrations up to 810 ppm by the end of the century. Precipitation in this area is almost exclusively concentrated in winter because of the passage of extratropical cold fronts. Rainfall amounts are most significant at high elevations (Favier et al. 2009) so rivers have a marked snowmelt regime with peak flow during spring/early summer and very low flows from late summer to late fall (Vicuña et al. 2011). Thus, the projected warming and drying trends should result in a significant decrease in annual mean streamflow, along with enhanced evapotranspirative demands, severely disrupting the agriculture in this already water-stressed area.

An estimation of climate-driven changes in the surface hydrology of Andean basins in semiarid Chile was conducted by Vicuña et al. (2011) using the water evaluation and planning (WEAP) model (Yates et al. 2005a). That modeling work targeted areas above 1,500 m above sea level within the Limarí River basin (30°S, Fig. 1), where streamflow records are largely unimpaired because of minimal agricultural development and very sparse population. When comparing end-of-century (2070–2100 under the A2 scenario) with present-day conditions (1960–1990), they find a 35–40% reduction of the annual mean volume, larger than the fractional precipitation decrease because of enhanced evaporation. They also found an earlier peak of the monthly streamflows leading to an extended dry season during summer and fall.

Downstream from the subbasins studied in Vicuña et al. (2011), waters from the Limarí basin irrigate more than 50,000 ha of highly productive agricultural land (due to its Mediterranean climate) and sustain the 100,000-inhabitant city of Ovalle and other minor towns (Fig. 1). In order to meet both farmers, and urban demands, an interconnected system of three reservoirs (Paloma, Recoleta, and Cogoti) was built during the first half of the twentieth century

<sup>1</sup>Centro Interdisciplinario de Cambio Global, Pontificia Universidad Católica de Chile, Santiago, Chile, Vicuña Mackenna 4860, Campus San Joaquín.

<sup>2</sup>Dept. of Civil Engineering, Facultad de Ciencias Físicas y Matemáticas, Universidad de Chile, Santiago, Chile; and Advanced Mining Technology Center, Facultad de Ciencias Físicas y Matemáticas, Universidad de Chile, Santiago, Chile (corresponding author). E-mail: jmcphoe@ing.uchile.cl

<sup>3</sup>Dept. of Geophysics, Facultad de Ciencias Físicas y Matemáticas, Universidad de Chile, Santiago, Chile; and Advanced Mining Technology Center, Facultad de Ciencias Físicas y Matemáticas, Universidad de Chile, Santiago, Chile.

Note. This manuscript was submitted on January 15, 2011; approved on October 6, 2011; published online on October 8, 2011. Discussion period open until February 1, 2013; separate discussions must be submitted for individual papers. This paper is part of the *Journal of Water Resources Planning and Management*, Vol. 138, No. 5, September 1, 2012. © ASCE, ISSN 0733-9496/2012/5-431-441/\$25.00.

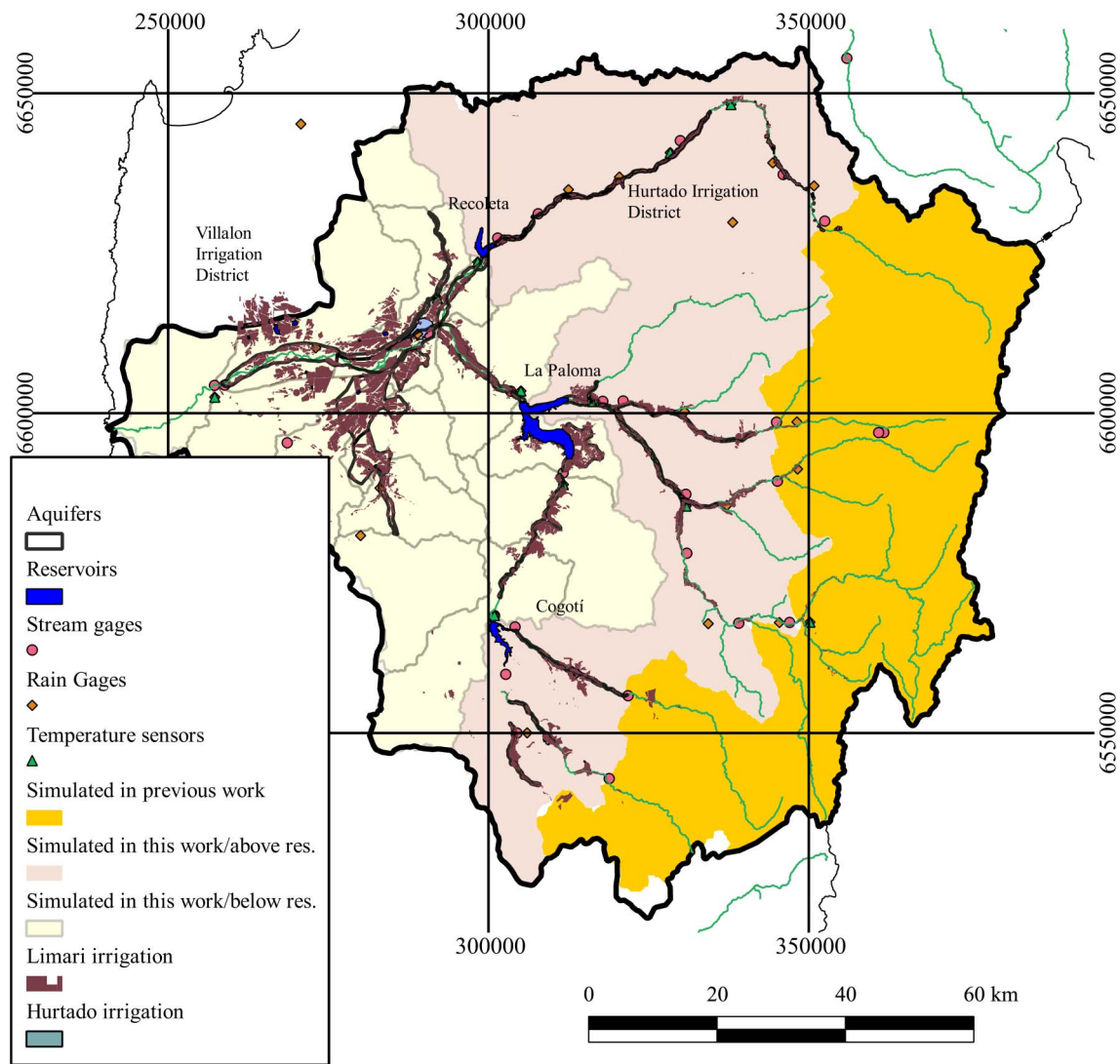


**Fig. 1.** Map of Limarí River basin showing monitoring stations (streamflow, precipitation, and temperature), reservoirs, and main water users in the basin including the city of Ovalle and irrigation districts; also shown are the upper watersheds simulated by Vicuña et al. (2011) and that served as starting point for the present work

(see Fig. 1 and Table 1 for reservoir characteristics). The system is capable of storing more than twice the volume of average annual runoff in the basin (about 400 million m<sup>3</sup>), thus acting as a buffer for the large El Niño Southern Oscillation-related inter annual variability that characterizes precipitation in this region (Montecinos and Aceituno 2003). In contrast, the Andean snowpack largely provides intra-annual regulation for basins in north-central Chile. Farmers downstream of the reservoirs benefit directly because the artificial storage allows them to have reliable water supplies through the year and even in dry years. Farmers upstream of reservoirs benefit indirectly because they are relieved (in most years) from their obligation of delivering water for downstream users. Upstream users, however, still suffer the effects of a variable climate and are more frequently unable to meet their irrigation demands than downstream farmers.

**Table 1.** Reservoir Characteristics

Variable	Reservoir		
	Recoleta	Paloma	Cogoti
Annual inflow (hm <sup>3</sup> )	77	243	83
Storage (hm <sup>3</sup> )	98	755	143

In the present study, the work of Vicuña et al. (2011) is extended and the change in the vulnerability—the ability to sustain a given level of agricultural activities—of farmers in the Limarí basin as a consequence of climate change is investigated. The Limarí basin is important for the Chilean economy in its own right, but this study also has relevance to other semiarid basins in Chile and elsewhere. The situation for those farmers located above reservoirs (without much adaptation capacity) has been considered separately from those farmers located below reservoirs. In both cases, annual irrigation demand coverage (defined as the ratio of total annual deliveries to annual irrigation requirements) is used as a vulnerability metric.

The WEAP model is used as the primary tool. In contrast with Vicuña et al. (2011), multiple simulations forced by different 30-year-long climate scenarios (current climate modified by a range of temperature and precipitation perturbations) are run. This delta approach [e.g., Vicuña and Dracup (2007)] allows the study of the sensitivity of agricultural vulnerability to climate regardless of the uncertainty inherent to the climate change conditions. Of course, particular emphasis is placed in the change in vulnerability associated with climate scenarios projected for the 21st century (either the next 30 years or the end of the century). An important

caveat is that agricultural coverage/usage and population have been kept as in present-day conditions, so the results are not predictions *sensu stricto* but only address the sensitivity of the current agricultural pattern to changes in the climate forcing.

## Model Development

The WEAP model (Yates et al. 2005a, b), a climate-driven hydrology and water resources model, is used to study the effects of climate-change projections on the hydrology and water resources of the Limarí River basin. In this section, an overview of the model development is provided and some results are shown in order to demonstrate that the calibration procedure resulted in a reasonable simulation of the present-day water cycle in the full Limarí basin, including supply and demand features. Furthermore, the present study builds on the modeling effort conducted by Vicuña et al. (2011) that used WEAP to simulate the hydrological conditions of the upper Limarí basin (Fig. 1, see also Table 6 in Vicuña et al. 2011).

## Basic Data

The model calibration requires knowledge of present-day climate (forcing), water demand, and the operating rules of the reservoir system. Historical meteorological conditions are obtained from a network of stations operated by the Chilean Water Directorate (DGA) within and around the Limarí basin (Fig. 1). Nine of these stations are used as index stations to distribute precipitation spatially, and two stations were used to provide temperature index data (Las Ramadas and Ovalle at the upper and lower sectors, respectively, Fig. 1 and Table 2). A set of streamflow-monitoring stations also operated by DGA is used to calibrate the semi-distributed, hydrologic module for different reaches of the river (Fig. 1 and

Table 3). Groundwater levels in the lower portions of the basin and operational characteristics of the reservoirs were obtained from CAZALAC (2006) and Dirección de Obras Hidráulicas (DOH) (Reglas de Operación Sistema Paloma, unpublished report, 2005), respectively.

Historical water demand was calculated on the basis of the spatial extent of cultivated land (CAZALAC 2006) apportioned among different crops using the Chilean farming census. Two major agricultural, irrigated districts are studied in detail. The Hurtado district (3,900 ha) is located in the upper part of the basin, upstream of the Recoleta reservoir (Fig. 1), obtaining its water directly and exclusively from the Hurtado River. The Villalon district (4,700 ha) is located in the lower section of the Limarí basin and has three possible sources of water: (1) the Recoleta reservoir through the Matriz Recoleta channel, (2) the Paloma reservoir through the Derivado Recoleta channel, and (3) groundwater supplies. As shown in Table 4, the area and crop distribution have changed over the last 20 years, especially in the more developed Villalon region. Irrigated

**Table 4.** Crop Mix Patterns (%)

Region	Crop	Year		
		1992	1997	2007
Irrigation region: Hurtado subbasin	Vegetables	14	3	4
	Pasture	41	42	46
	Orchards	30	23	31
	Vineyards	10	32	18
	Cereals	5	1	1
Irrigation region: Canal Villalon	Vegetables	17	17	8
	Pasture	11	53	44
	Orchards	3	13	32
	Vineyards	3	15	13
	Cereals	65	3	3

**Table 2.** Meteorological Stations Used as Index Stations in Distribution Model

Section	Station	Variable	Elevation (m)	Latitude	Longitude
Upper	Pabellon (PA)	Precipitation	1,920	30°24'40"S	70°33'15"W
	Las Ramadas (LR)	Precipitation, temperature	1,380	31°01'05"S	70°35'08"W
	Tascadero (TA)	Precipitation	1,230	31°00'55"S	70°39'59"W
	Cogoti 18 (C18)	Precipitation	840	31°05'01"S	70°57'00"W
Intermediate	Tome (TO)	Precipitation	420	30°49'00"S	70°58'00"W
	Embalse Recoleta (ER)	Precipitation	350	30°30'24"S	71°05'59"W
	Embalse Paloma (EP)	Precipitation	320	30°41'35"S	71°02'10"W
Lower	Punitaqui (PU)	Precipitation	280	30°49'23"S	71°15'29"W
	Ovalle (OV)	Precipitation, temperature	220	30°36'00"S	71°12'00"W

**Table 3.** Streamflow Gauging Stations

Section	Station	Surface area (km <sup>2</sup> )	Elevation (m)	Latitude	Longitude
Upper	Hurtado, San Agustín (HSA)	656	2,035	30°27'00"S	70°32'00"W
	Los Molles, Ojos de Agua (LOJ)	144	2,355	31°45'00"S	70°27'00"W
	Mostazal, Cuestecita (MCU)	353	1,250	30°49'00"S	70°37'00"W
	Grande, Las Ramadas (GLR)	544	1,380	31°01'00"S	71°36'00"W
	Tascadero, Dsesemboadura (TDE)	238	1,370	31°01'00"S	70°41'00"W
	Cogoti, Fragueta (CFR)	475	1,065	31°07'00"S	70°52'00"W
	Intermediate	Hurtado, Angostura (HAN)	1,810	500	30°26'00"S
Rapel, Junta (RJu)		828	485	30°42'00"S	70°52'00"W
Mostazal, Caren (MCA)		591	700	30°50'00"S	70°46'00"W
Grande, Puntilla San Juan (GPS)		3,521	420	30°42'00"S	70°55'00"W
Cogoti, Entrada Embalse (CEM)		735	670	31°01'00"S	71°03'00"W
Lower		Limari, Panamericana (LPA)	11,261	165	30°40'00"S

areas and crop fractions between census years were linearly interpolated for use in WEAP.

### Model Calibration Upstream from Reservoirs

The model development started with watersheds located upstream of the reservoirs but downstream of those simulated in Vicuña et al. (2011) (see Fig. 1), so some of the basins simulated here have a sizable amount of land dedicated to agriculture. Land use was classified into different categories and assigned an initial set of physical parameters to be used in the hydrologic module. Precipitation historical time series (monthly values) for each of these intermediate watersheds were derived on the basis of the index stations using the hybrid logarithmic-isohyetal method proposed in Vicuña et al. (2011). Temperature time series at each watershed were computed by using an index station and a monthly vertical temperature gradient; the value at the station was augmented or reduced by the product of the vertical gradient and the difference of the watershed mean elevation and the index station elevation. Other key parameters in the model setup include upper and lower irrigation soil moisture thresholds, which define a range of desirable soil moisture values for each crop. Soil moisture falling below the lower threshold triggers an irrigation requirement that ceases when soil moisture reaches the upper threshold (Purkey et al. 2008).

Parameter calibration was made in an iterative fashion until reaching a good agreement between the observed and simulated monthly streamflow at the five stations located above the reservoirs. In all cases, the actual monthly mean time series was used as the basis of the calibration. As an example, Fig. 3 shows the long-term-mean annual cycle and Fig. 2 shows monthly mean time series of streamflow in three stations. The simulated mean annual cycle exhibits a double hump in agreement with the observations, as expected from hydrologic conditions being influenced by both precipitation in winter (June, July, August) and snowmelt in spring

(September, October, November) and summer (December, January, February). WEAP also represents properly most of the actual monthly values except for some underestimation (overestimation) during periods of low (high) flow. The good performance of WEAP in simulating monthly stream flow time series in the upper Limarí basin is further supported by the values of two goodness-of-fit statistics, the Nash-Sutcliffe (0.7–0.9) and bias score (between –11 to 2.5%) obtained in the different stations (see also Fig. 3).

### Model Calibration below Reservoirs

The second phase in the model development involved the lower sections of the Limarí basin, including water demand from more than 20 irrigation districts (<40,000 ha) and the 100,000-inhabitant city of Ovalle, Chile. The water input is streamflow from the above-reservoir basins (already calibrated) and precipitation over the lower sections. Surface water deliveries to these demand sites are made by a complex system of canals draining water stored in the three main reservoirs within the basin (Paloma, Recoleta, and Cogoti, Table 1 and Fig. 1). Thus, the development and calibration of the model in this lower section requires appropriate representation of both demand and supply features, including irrigation returns and water-release decisions from the interconnected system of reservoirs. The operating rules, in use since 1988, describe the amount of water that can be withdrawn from any reservoir in a given water year (DOH, Reglas de Operacion Sistema Paloma, unpublished report, 2005). Depending on the volume of water stored in all three reservoirs (VT), the rules are

- If  $VT \geq 1,000 \text{ hm}^3$ , then deliver without restriction;
- If  $500 \leq VT < 1,000 \text{ hm}^3$ , deliver a maximum of  $320 \text{ hm}^3$ ;
- If  $VT < 500 \text{ hm}^3$ , deliver up to half of stored water.

Under conditions of severe surface water shortage, most demand sites may also rely on groundwater extractions, altering

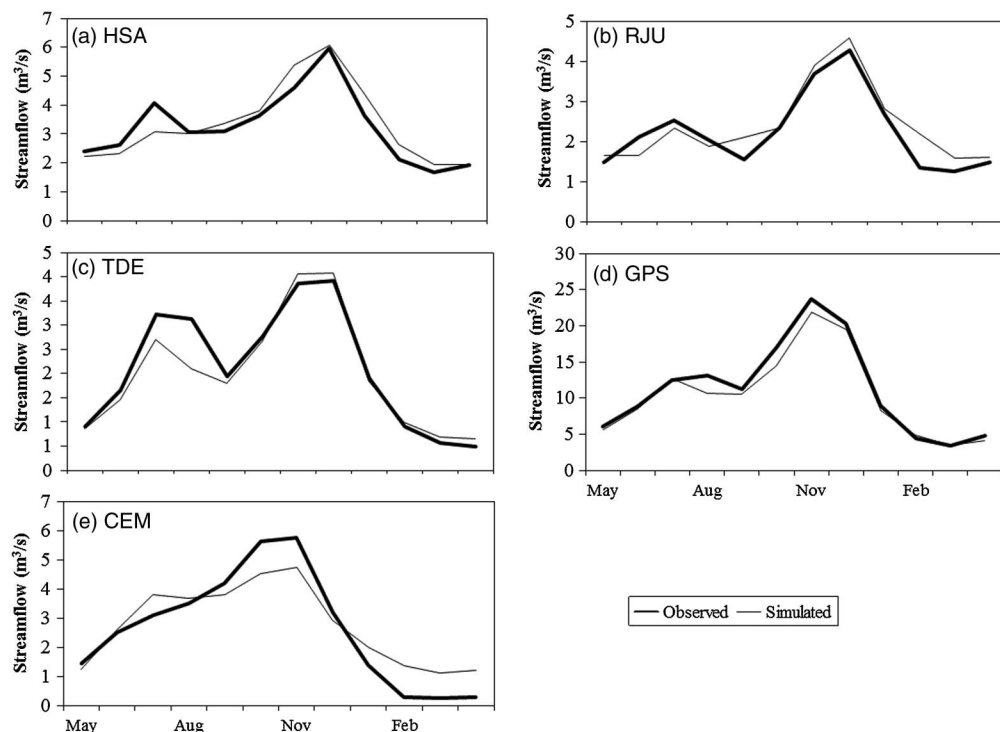


**Fig. 2.** Observed (thick line) and WEAP-simulated (thin line) long-term monthly mean streamflow at five stations in the intermediate reaches of the Limarí basin

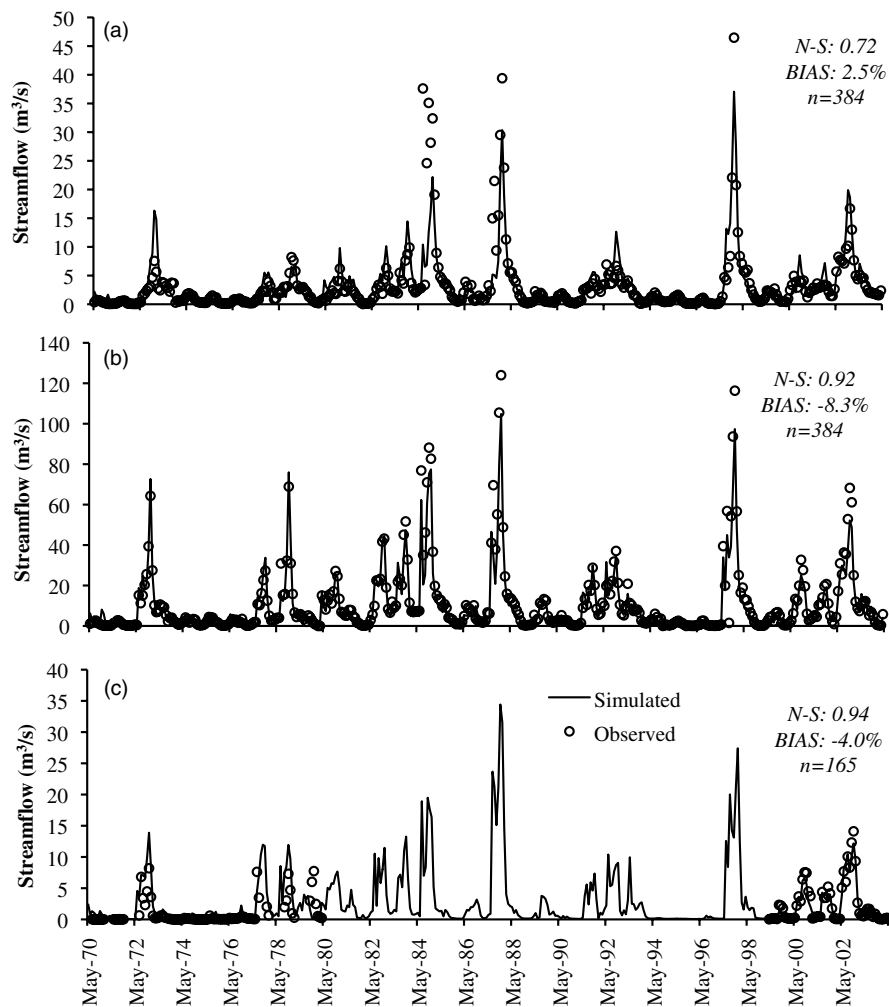


**Fig. 3.** Observed (dots) and WEAP-simulated (line) monthly streamflow time series for the calibration period at three stations in the middle Limarí basin; each station's name and two fit statistics (Nash-Sutcliffe and bias) are indicated; the number of data points used in this calibration ( $n$ ) is also included in each panel

the hydrological response in the final reaches of the river. A set of lumped representations of aquifers was included in the lower sections of the basin in which farmers are allowed to use groundwater as a secondary source of water, limited by pumping capacity.

Results from the calibration are encapsulated in a series of key figures and two fits statistics (Nash-Sutcliffe and bias) based on the monthly time series at each station (number of data points also indicated in each figure). Fig. 4(a) shows the monthly volume of the Paloma reservoir, from which it is apparent that the model generally represents drawdown/refill periods during dry/wet years. Similar results are obtained for the other two reservoirs; in each case, the correlation coefficient between observed and simulated monthly mean reservoir storage is greater than 0.8. Fig. 4(b) shows the simulated monthly groundwater levels at the Camarico aquifer and dynamic levels measured at a pumping well. Although the representation of aquifers in WEAP is very simple (Yates et al. 2005a), the model was able to reproduce well the magnitude of the aquifer response during the historical period, except for a shorter than observed recovery time after the extremely dry year of 1997. Stream-aquifer interactions also seem to be reasonably simulated when comparing simulated and observed monthly streamflow time series at the basin outlet (LPA station, Fig. 5). Streamflow at that location is highly skewed with very low flows most of the time, interrupted

by a few high flows in the wettest years. Despite the clear challenges in representing such an extreme hydrologic regime with a simple hydrologic model, Fig. 5 shows a reasonable calibration for this stream gauge.

It has been demonstrated in this section that, after a stepwise, trial-and-error calibration procedure, the WEAP model represents reasonably well water demand and supply in the entire Limarí basin under current climate conditions and historical crop patterns/reservoir operation. In the next sections, the calibrated model is taken advantage of to explore the sensitivity of hydrological conditions and agriculture vulnerability to climate change.

### Future Climate Scenarios and Modeling Strategy

Climate projections for central Chile based on general circulation models (GCMs) consistently show warming and drying trends throughout the 21st century [e.g., Christensen et al. (2007)]. Nevertheless, at least three main sources of uncertainty remain in future climate projections. First and foremost, future greenhouse gas (GHG) emissions are unknown, as reflected in a wide range of equally probable emission scenarios (Nakicenovic and Stewart 2000). There is also variability in the magnitude of the regional climate changes among the over 20 available GCM outputs because

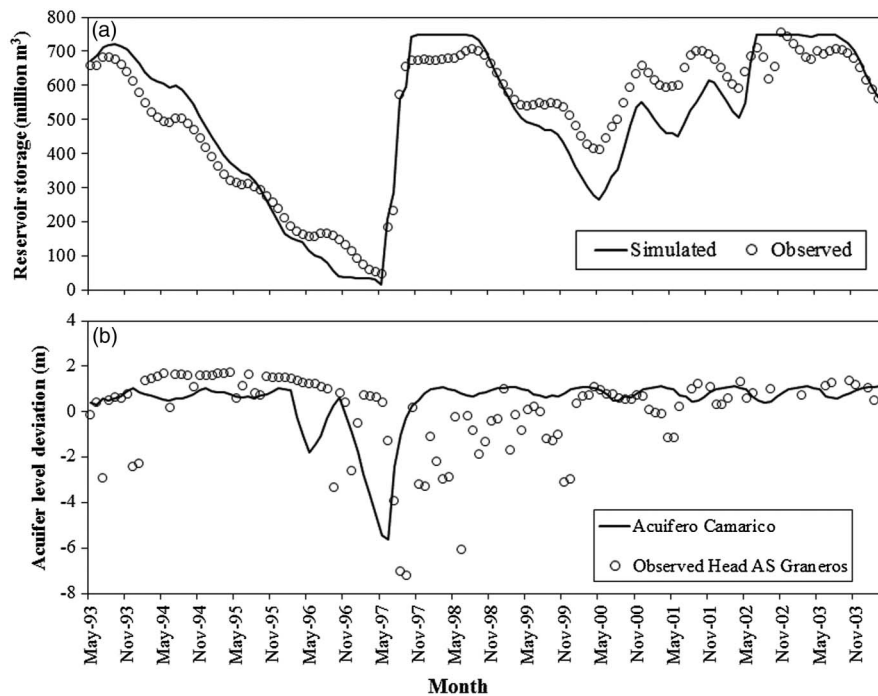


**Fig. 4.** (a) Observed (dots) and WEAP-simulated (line) monthly storage at La Paloma reservoir for calibration period; (b) observed (dots) and WEAP-simulated (line) monthly aquifer level deviations at Camarico for calibration period

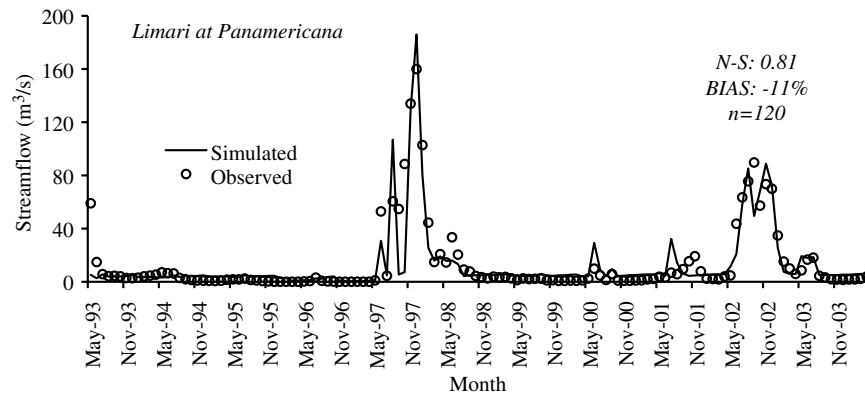


**Fig. 5.** Observed (dots) and WEAP-simulated (line) monthly streamflow at station LPA close to the basin's outlet for calibration period; two fit statistics (Nash-Sutcliffe and bias) are included; the number of data points used in this calibration ( $n$ ) is also included

of the intermodel differences in dynamical cores and parameterization of radiative transfer. Finally, because of the special physiographic characteristics of watersheds on the western slope of the Andes cordillera (steep, short river lengths, with an over 3 elevation gain from the Pacific Ocean in less than 200 km), the spatial scale of current GCM modeling grids is inadequate to assess local effects on the hydrologic regime, and downscaling approaches (statistical or dynamical) introduce an additional layer of uncertainty. Indeed, climate changes observed in Chile during the last three decades exhibit considerable altitudinal and latitudinal dependence, which is hardly resolved by the current generation of GCM (Falvey and Garreaud 2009).

To illustrate the level of uncertainty in climate change projections for the Limarí basin, Fig. 6 shows the changes in temperature

( $dT = T_{\text{future period}} - T_{\text{base-line}}$ , horizontal axis) and changes in precipitation normalized by the current climate precipitation average ( $dP_f = 100 \times dP / P_{\text{base-line}}$ , vertical axis) simulated by each of the GCMs that participated in the Intergovernmental Panel on Climate Change (IPCC) fourth assessment report (i.e., the World Climate Research Programme's phase 3 of the Coupled Model Intercomparison Project multimodel database). The values shown are unscaled GCM outputs bilinearly interpolated to the location of the LR meteorological station. The figure includes results for three GHG emission scenarios (B1 = low, CO<sub>2</sub> concentrations up to 530 ppm by 2100; A1b = medium, CO<sub>2</sub> concentrations up to 705 ppm by 2100; and A2 = high, CO<sub>2</sub> concentrations up to 810 ppm by 2100) and two future time periods (2010–2040 and 2070–2100). For the 2010–2040 period, all GCM projections

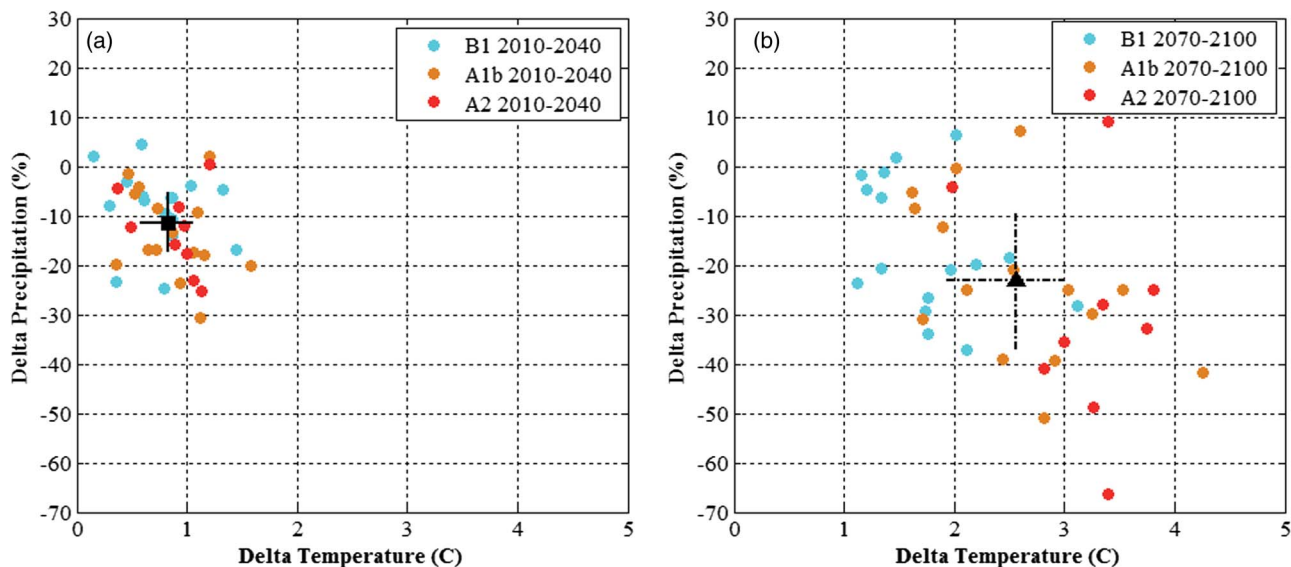


**Fig. 6.** Temperature (horizontal axis) and precipitation (relative to current values, vertical axis) change projections at LR meteorological station in the Limarí basin these projections were interpolated from a set of GCMs used in the latest IPCC report (Christensen et al. 2007); (a) projections for 2010–2040 under the B1, A1b, and A2 emission scenarios; the square marker is the multimodel, multisenario mean  $dT$  and  $dP_f$  projections for this near-future period; (b) projections for 2070–2100 under the B1, A1b, and A2 emission scenarios; the triangle marker is the multimodel mean  $dT$  and  $dP_f$  projections for this far-future period; in both panels, the horizontal and vertical lines crossing each marker represent the range of potential  $dT$  and  $dP_f$  projections that cover a 50% likelihood around the mean projections

cluster around  $dT \approx +0.5^\circ\text{C}$  and  $dP_f = -10$  to  $-30\%$ . Model projections tend to diverge as they move far in the future and under the high emission scenario (A2), when  $dT = +1$  to  $+4^\circ\text{C}$  and  $dP_f = -15$  to  $-50\%$ .

In light of these uncertainties, the delta (or sensitivity) approach was adopted to understand the implications of climate change on the Limarí basin water resources. Instead of using direct or down-scaled GCM outputs, new 30-year-long time series of monthly precipitation and temperature were created by modifying the historical time series by a discrete set of changes ( $dP_f$  and  $dT$ ) applied equally to all months. Here 10 scenarios of increasing temperature levels from  $0^\circ\text{C}$  to  $+5^\circ\text{C}$ , every  $0.5^\circ\text{C}$ , and 25 scenarios of changing precipitation from  $-30\%$  to  $+30\%$ , every  $2.5\%$  have been considered. Subsequently, these  $10 \times 25$  combined scenarios were used to force the WEAP model during hypothetical 30-year periods. Recall, however, that the land-use and reservoir operating rules were kept at their current state.

The delta approach allows analyzing multiple GCM simulations in order to assess water resources sensitivity to climate change (Revelle and Waggoner 1983; Gleick 1987; Jeton et al. 1996; Miller et al. 2003, see review in Vicuña and Dracup 2007). This methodology, however, doesn't allow exploring the effects of future changes in the seasonal cycle and/or interannual variability of climate forcing because the approach relies on the same sequence of hydrologic conditions that occur under historical conditions.

## Results

### Upper Basin Hydrological Changes

A summary of the hydrological sensitivity to climate change is presented in Fig. 7 for the Hurtado subbasin, an important watershed located above the Limarí's reservoirs. For each of the new climate scenarios, the changes in the annual mean runoff (average of 30 years), expressed as a percentage of the baseline mean value

( $dQ_f$ ) and the hydrograph centroid timing (the day when the center of mass of the annual hydrograph occurs) measured as days of deviation from the baseline case are shown. As expected, a decrease (increase) in precipitation leads to a reduction (increase) in annual mean runoff, and an increase in temperature leads to an earlier centroid. Nevertheless,  $dQ_f$  is not identical to  $dP_f$  even for the case with no temperature change, signaling weak nonlinear hydrological processes within the basin. Furthermore, an increase in temperature also leads to a weak but sizable reduction in annual mean runoff ( $-10\%$  for  $dT = 5^\circ\text{C}$ ) because of enhanced evaporation in a warmer climate, and a reduction (increase) in precipitation leads to an earlier (delayed) hydrograph centroid. Both cross effects become stronger in higher elevation subbasins (not shown), as analyzed in Vicuña et al. (2011).

When considering the most likely regional climatic changes in the next 30 years (cf. Fig. 7), a reduction in annual runoff is projected on the order of 20% with respect to current values and approximately a week earlier hydrograph centroid. For the end of the century period (2070–2100 under scenario A1b),  $dQ_f$  is obtained in the range of 30–40% and about a half a month earlier hydrograph centroid, consistent with the results in Vicuña et al. (2011) for the upper Limarí basin. As shown next, these near- and far-future changes could have profound impacts on the appropriate use of water for different farmers in the basin.

### Agriculture Vulnerability

Agriculture vulnerability is quantified here by the ratio of total annual deliveries to annual irrigation requirements and referred to as annual irrigation coverage. Results are presented and discussed for two key irrigation districts: Hurtado (upstream of the reservoirs) and Villalon (downstream of the reservoirs). Fig. 8 shows the 30-year average of annual irrigation coverage as a function of  $dT$  and  $dP_f$  for the Hurtado and Villalon subbasins. Baseline irrigation coverage ( $dT = 0$  and  $dP_f = 0$  in Fig. 8) is 88% in Hurtado and 95% in Villalon.

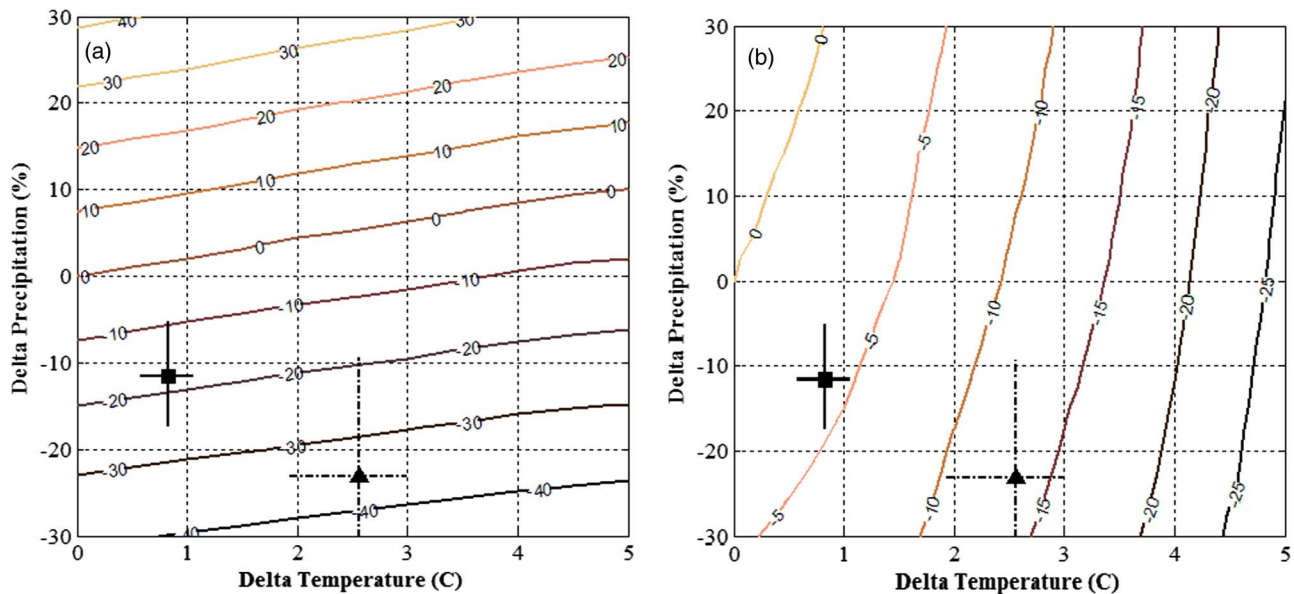


**Fig. 7.** (a) WEAP-simulated changes in annual runoff (measured as percent change from base runoff) at station HAN as function of temperature (horizontal axis) and precipitation (vertical axis) changes; the multimodel, multiscenario mean  $dT$  and  $dPf$  projected at LR is shown with the square marker for the period 2010–2040 and the triangle marker for the period 2070–2100 under scenario A1B; (b) as panel (a) but for the WEAP-simulated hydrograph timing (measured as number of days from base location of centroid) at station HAN; in both panels, the horizontal and vertical lines crossing each marker represent the range of potential  $dT$  and  $dPf$  projections that cover a 50% likelihood around the mean projections

In both basins, a drier ( $dPf < 0$ ), warmer ( $dT > 0$ ) climate results in a decrease in irrigation coverage because of the superposition of three effects: (1) reductions in the amount of water for irrigation available in the river (reduced supply), (2) increased demand at the plot scale due to enhanced evapotranspiration (temperature effect), and (3) reduced soil moisture (precipitation effect). The farmers' vulnerability is, however, dependent on whether their district is located upstream or downstream of the reservoirs. Consider first the case  $dPf = -30\%$  and  $dT = 0^\circ\text{C}$  because irrigation coverage is strongly dependent on precipitation. The absolute reduction in irrigation coverage is 20% in the Hurtado basin (from 88% coverage curve to 68% coverage curve, approximately), twice the reduction in the Villalon basin (from more than 95% coverage to more than 85% coverage). Similar results emerge when considering the climate change projected for the near future. In the Hurtado subbasin, the coverage decreases approximately 10% for the 2010–2040 period and 25% for the end of the century. In the Villalon subbasin, the coverage only decreases approximately 3% in the near-future period and 8% for the end of the century.

Farmers downstream (upstream) of reservoirs are thus less (more) vulnerable to climate changes. Although reservoir inflows are reduced both with an increase in temperature and a reduction in precipitation, the multiyear carrying capacity of the reservoir system provides enough surplus storage to allow demand satisfaction during dry year sequences.

### Changes in Water Supply Operations

Variations in water supply and demand result in changes to how the reservoir's system behaves (recall that the operating rules were kept at current status). Fig. 9(a) shows the changes in annual average storage (relative to current conditions) for the La Paloma reservoir; qualitatively similar results are obtained for the Recoleta and Cogoti reservoirs. Two features stand out: first, the system today is very close to its maximum capacity because any significant

increase in precipitation only produces a modest increase in average storage (although it results in enhanced spills from each reservoir), while a significant reduction in precipitation leads to an even larger reduction in average storage. The second feature to note is the significant effect that temperature has on average storage. For example, in order to compensate for the water cycle losses due to a  $5^\circ\text{C}$  temperature increase, there needs to be a 30% precipitation increase. Because there is no sublimation modeling and there are no large aquifers in the upper watersheds, the only possible loss from the water cycle as considered in the model at this height is evapotranspiration, which is affected by temperature. A further explanation on these issues is given in Vicuña et al. (2011). Considering the climate change projected for the next 30 years, the model in this paper suggests reductions of about 15, 10, and 15% in average storage at La Paloma, Cogoti, and Recoleta, respectively [only results for the Paloma reservoir are shown in Fig. 9(a)]. The average storage in these reservoirs further decreases to 30, 35, and 35% when considering the climate change projections for the last 30 years of the 21st century.

Climate change can also alter the occurrence of large inflows to the reservoirs. Although a monthly time step model is not the proper tool for extreme event analysis, Fig. 9(b) presents a proxy for this type of effects by looking at relative changes in the maximum monthly inflow (relative to current conditions) to La Paloma reservoir over the simulation period. As expected, the maximum inflow has a strong and positive dependence on precipitation. The sensitivity to changes in temperature, however, depends on the magnitude of  $dT$ . For modest changes ( $dT < 1^\circ\text{C}$ ), a reduction in large inflows, likely due to an increase in water demand in spring/summer months when the largest flows occur today, is seen. A larger increase in temperature, however, leads to an increase in large inflows relative to current climate (the threshold for this differential behavior depends on the concomitant change in precipitation). It is inferred that the larger maximum inflows are due to winter storms encompassing a much larger pluvial area (and reduced snow area) because of the warmer conditions that raise

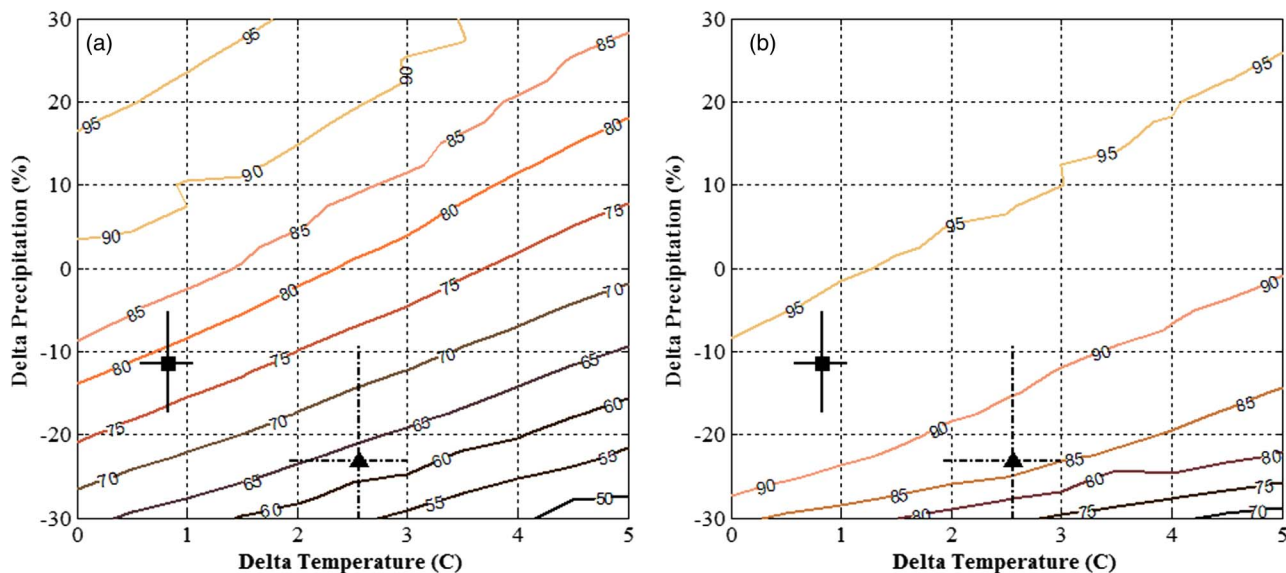


**Fig. 8.** WEAP-simulated annual irrigation demand coverage (values represent percentage based on nominal annual demand volume) for users associated with (a) Hurtado subbasin and (b) canal Villalón as a function of temperature (horizontal axis) and precipitation (vertical axis) changes; the marker and lines indicate the projected dT and dP as explained in Fig. 6 under scenario A1B

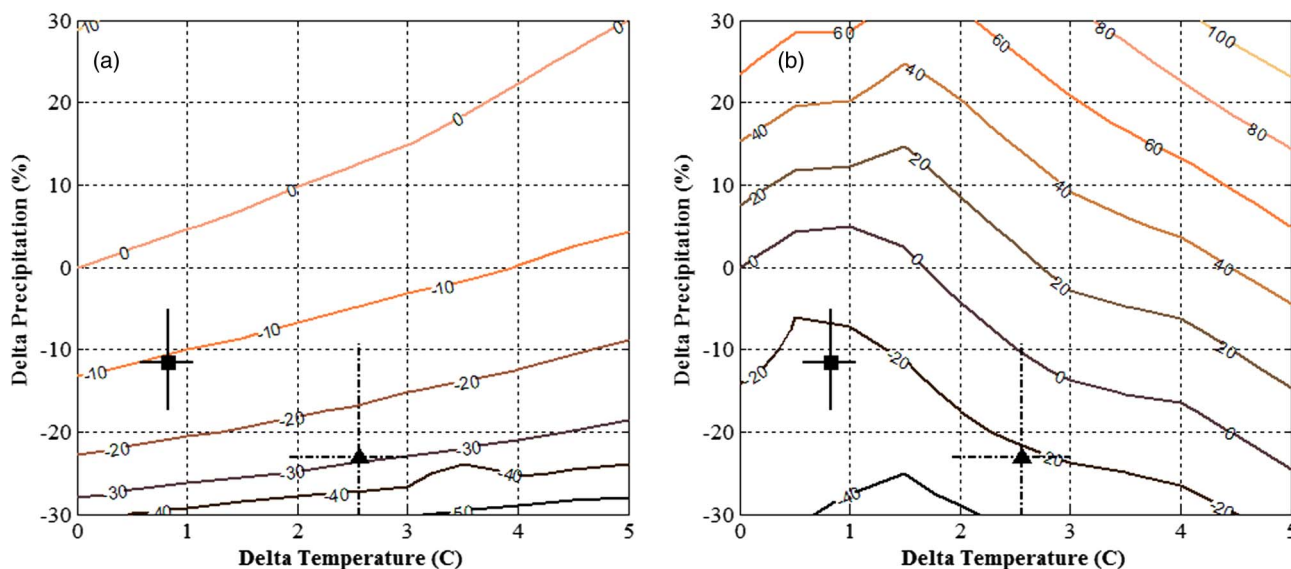


**Fig. 9.** (a) WEAP-simulated changes in annual average storage (measured as percent change from base storage) and (b) WEAP-simulated changes in maximum inflow to reservoir (measured as percent change from historic maximum inflow) at La Paloma reservoir as a function of temperature (horizontal axis) and precipitation (vertical axis) changes; the square marker is the multimodel, multiscenario mean dT and dP projected at LR for the period 2010–2040; the triangle marker is the multimodel mean dT and dP projections for LR for the period 2070–2100 under scenario A1B; in both panels, the horizontal and vertical lines crossing each marker represent the range of potential dT and dP projections that cover a 50% likelihood around the mean projections

the 0°C isotherm in the Andean basins. In any case, for the climate changes projected for the 2010–2040 period, the model in this paper suggests a reduction in large inflows to Paloma/Cogoti/Recolta on the order of 20/15/20%, respectively [only Paloma reservoir inflows are presented in Fig. 9(b)].

Farmers in the lower sections of the Limarí basin rely mostly on stored water in the reservoir system, but some of them have an alternative supply based on groundwater pumping; the use of this resource could become more frequent under warmer/drier conditions. To explore this effect, Fig. 10 shows the simulated time series

of stored water at La Paloma reservoir (surface water supply) and Camarico aquifer water level (groundwater supply) for current conditions and two sensitivity scenarios. Groundwater is a secondary source (or not used at all) if enough supply from the reservoir is available (e.g., dT = 0°C, dP = 30%). However, in the extreme pessimistic scenario (dT = +5°C, dP = -30%), the reservoir storage drops significantly, extending the drought year of 1997 for two more years. In the simulated operation of the system, farmers compensate for this reduced surface supply by relying on groundwater pumping, which results in greatly reduced aquifer

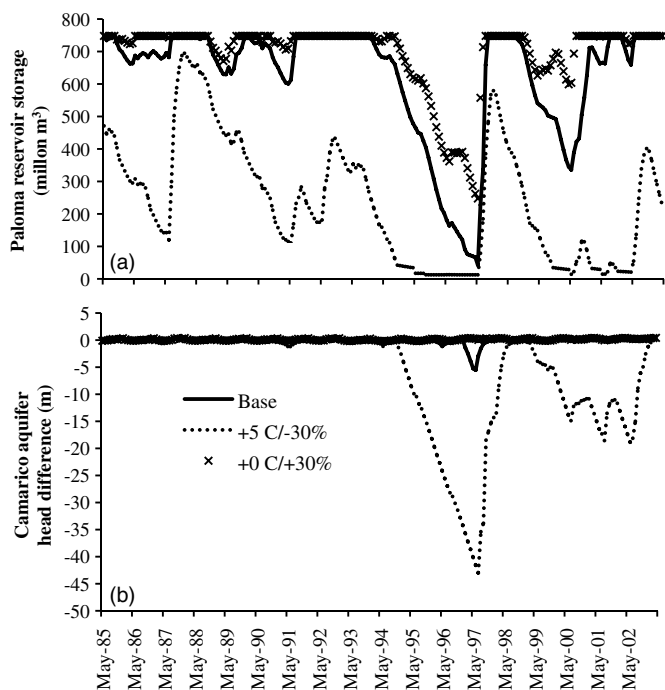


**Fig. 10.** Monthly time series under two extreme scenarios:  $dT = 0^{\circ}\text{C}$ ,  $dPf = 30\%$  (solid line), and  $dT = +5^{\circ}\text{C}$ ,  $dPf = -30\%$  (dashed line) for (a) the La Paloma reservoir storage and (b) the Camarico aquifer head difference; the base line (current climate) is included using crosses

levels. On the other hand, the aquifer is able to recover in only a few years under this scenario, returning to an almost-full condition after 2 years.

Fig. 11 shows the sensitivity of water flows at LPA, just a few kilometers from the Pacific Ocean, where all water supply and demand effects throughout the basin are compounded. Water outflows from the basin are sensitive to different climate scenarios. Considering the warming/drying trend projected during this century, there could be an approximately 40% reduction in water flowing in the lower reaches of the basin for the 2010–2040 period, and a more than 60% reduction by the end of the century under the A1b scenario. Fig. 11 also reveals the aggregated effect on streamflow of temperature and precipitation. For the constant temperature case ( $dT = 0^{\circ}\text{C}$ ),  $dQ_f = 2 \times dPf$ , and for the constant precipitation case ( $dPf = 0$ ),  $dQ_f$  was obtained as being between 2 and 6%/°C, nearly twice the sensitivity in the upper part of the basin (cf. Fig. 7). This added sensitivity to climate change is likely the result of nonlinearities associated with irrigation in the lower reaches of the basin. In order to preserve as much land under irrigation as possible, diversion from the river (of water previously stored in reservoirs) does not follow the same variations as expected from climate changes. The result is an exaggerated sensitivity of streamflow at the outlet of the basin. This outcome of the model provides a further insight on issues that have to be taken into account when analyzing vulnerability and adaptation to climate change.

## Concluding Remarks

In this work, a sensitivity approach to assess the vulnerability of the existing storage and distribution infrastructure under climate projections in the Limarí river basin, a snowmelt driven basin in semiarid northern Chile ( $30^{\circ}\text{S}$ ) is presented. This approach provides a good platform from which to understand some of the key effects of

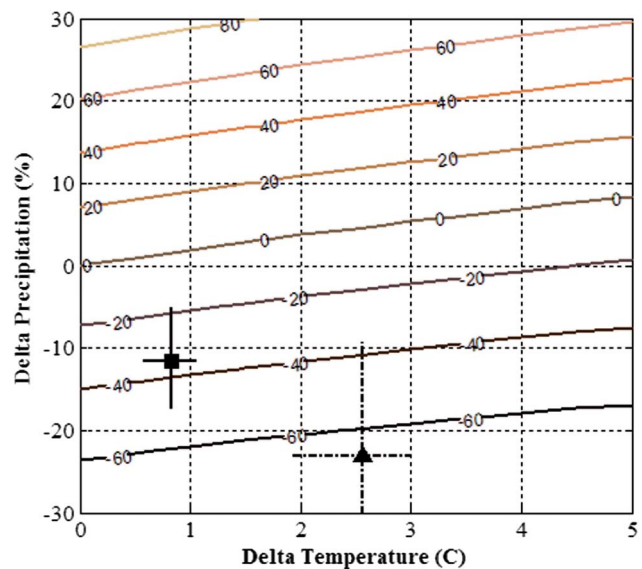


**Fig. 11.** WEAP-simulated changes in outflow from the basin (measured as percent change from base annual streamflow at LPA monitoring station) as function of temperature (horizontal axis) and precipitation (vertical axis) changes; the multimodel, multisenario mean  $dT$  and  $dPf$  projected at LR under scenario A1B is shown by the square marker for the period 2010–2040 and the triangle marker for the period 2070–2100; in both panels, the horizontal and vertical lines crossing each marker represent the range of potential  $dT$  and  $dPf$  projections that cover a 50% likelihood around the mean projections

climate change at the basin scale and provides an adequate framework to study future adaptation strategies and long-term policies (e.g., large irrigation infrastructure development policies).

The projected drying and warming trends reduce the supply and increase the demand of water in the basin, leading to a complex situation for water resources management. The existence of the Limarí reservoirs and channel network, however, will buffer some of the implications of near term climate change for agricultural districts located downstream of the reservoirs. Even while working at much lower average storage levels, reservoirs are able to sustain high percentages of demand coverage under quite severe climate projections.

Despite the inclusion of a simple groundwater representation, it is possible to infer from modeling results that future climate scenarios indicate an increased use of groundwater for irrigated agriculture, and hence, much larger fluctuations in aquifer levels. Large, long-lasting depressions can be detrimental to the environment in which aquifers exist in fragile equilibrium and sustain threatened ecosystems such as wetlands. On the other hand, the more intense use of aquifers as an underground reservoir could mitigate greatly the effects of climate change and provide effective adaptation strategies to users in semiarid regions, but it requires a more informed and active management of these resources.

The projections shown in this paper call for the analysis of long-term adaptation policies in these basins including hard (infrastructure) and also soft solutions such as water market enhancements and integrated basin water management. Future work includes a more realistic representation of farmers' behavior. It is expected that under changes in climate conditions, crop patterns could be altered due to relative changes in crop productivities and changes in water supply availability for irrigation. Also, some features of basin management remain to be solved in a more general framework that was beyond the scope of this work. Examples of potential

improvements include a better simulation of groundwater dynamics or other environmentally sensitive variables such as water quality in the lower sections of the basin where streamflow volume can be reduced as much as 60% during the present century.

## Acknowledgments

The authors would like to acknowledge the help given in the development of this model by representatives of different water institutions in the Limarí basin such as the Sistema Paloma Management, Junta Vigilancia del Rio Grande y Limari, Junta de Vigilancia del Rio Hurtado, Asociacion de Canalistas del Embalse Recoleta and Asociacion de Canalistas del Embalse Cogoti. The work also benefited from the generous insights of Francisco Meza and Guillermo Donoso. This work was partially funded by PBCT CONICYT (Chile) grants ACT-19/Redes-9 and with the aid of FONDECYT throughout Grant 1110297.

## References

- Centro del Agua para Zonas Aridas y Semiaridas de America Latina y El Caribe (CAZALAC). (2006). "Aplicación de metodologías para determinar la eficiencia de uso del agua estudio de caso en la región de Coquimbo." Elaborado por CAZALAC; con la asesoría de RODHOS Asesorías y Proyectos Ltda; Gobierno Regional—Región de Coquimbo.
- Christensen, J. H. et al. (2007). "Regional climate projections." *Climate change 2007: The physical science basis*, Cambridge University Press, New York.
- Falvey, M., and Garreaud, R. D. (2009). "Regional cooling in a warming world: Recent temperature trends in the southeast Pacific and along the west coast of subtropical South America (1979–2006)." *J. Geophys. Res. D: Atmos.*, 114, D04102.
- Favier, V., Falvey, M., Rabatel, A., Praderio, E., and López, D. (2009). "Interpreting discrepancies between discharge and precipitation in high-altitude area of Chile's Norte Chico region (26–32°S)." *Water Resour. Res.*, 45, W02424.
- Fuenzalida, H., Aceituno, P., Falvey, M., Garreaud, R., Rojas, M., and Sanchez, R. (2007). "Study on climate variability for Chile during the 21st century." Technical report prepared for the National Environmental Committee (in Spanish) (<http://www.dgf.uchile.cl/PRECIS>) (Jan. 2011).
- Gleick, P. H. (1987). "Regional hydrologic consequences of increases in atmospheric CO<sub>2</sub> and other trace gases." *Clim. Change*, 10(2), 137–161.
- Held, I. M., and Soden, B. J. (2006). "Robust responses of the hydrological cycle to global warming." *J. Clim.*, 19(21), 5686–5699.
- Jeton, A. E., Dettinger, M. D., and Smith, J. L. (1996). "Potential effects of climate change on streamflow: Eastern and western slopes of the Sierra Nevada, California and Nevada." *Water Resources Investigations Rep. 95-4260*, U.S. Geological Survey, Washington, DC.
- Miller, N. L., Bashford, K. E., and Strem, E. (2003). "Potential impacts of climate change on California hydrology." *J. Am. Water Resour. Assoc.*, 39(4), 771–784.
- Montecinos, A., and Aceituno, P. (2003). "Seasonality of the ENSO-related rainfall variability in central Chile and associated circulation anomalies." *J. Clim.*, 16(2), 281–296.
- N. Nakicenovic and R. Swart, eds. (2000). *Special report on emissions scenarios*, Cambridge University Press, New York.
- Purkey, D. et al. (2008). "Robust analysis of future climate change impacts on water for agriculture and other sectors: A case study in the Sacramento Valley." *Clim. Change*, 87, 109–122.
- Revelle, R. R., and Waggoner, P. E. (1983). "Effects of a carbon dioxide induced climatic change on water supplies in the western United States." *Changing Climate*, National Academy of Sciences Press, Washington, DC.
- Vicuña, S., and Dracup, J. A. (2007). "The evolution of climate change impact studies on hydrology and water resources in California." *Clim. Change*, 82(3–4), 327–350.
- Vicuña, S., Garreaud, R., and McPhee, J. (2011). "Climate change impacts on the hydrology of a snowmelt driven basin in semiarid Chile." *Clim. Change*, 105(3), 469–488.
- Yates, D., Sieber, J., Purkey, D., and Huber-Lee, A. (2005a). "WEAP21: A demand-, priority-, and preference-driven water planning model: Part 1, model characteristics." *Water Int.*, 30(4), 487–500.
- Yates, D., Sieber, J., Purkey, D., Huber-Lee, A., and Galbraith, H. (2005b). "WEAP21: A demand-, priority-, and preference-driven water planning model: Part 2, Aiding freshwater ecosystem service evaluation." *Water Int.*, 30(4), 501–512.